

LIBRARY  
ROYAL AIRCRAFT ESTABLISHMENT  
BEDFORD.

R. & M. No. 3169  
(18,943)  
A.R.C. Technical Report



MINISTRY OF AVIATION

AERONAUTICAL RESEARCH COUNCIL  
REPORTS AND MEMORANDA

# The Effect of Structural Damping on Binary Flutter

*By*

E. G. BROADBENT and MARGARET WILLIAMS

© *Crown copyright 1960*

LONDON: HER MAJESTY'S STATIONERY OFFICE

1960

EIGHT SHILLINGS NET

# The Effect of Structural Damping on Binary Flutter

By

E. G. BROADBENT and MARGARET WILLIAMS

COMMUNICATED BY THE DEPUTY CONTROLLER AIRCRAFT (RESEARCH AND DEVELOPMENT)  
MINISTRY OF AVIATION

---

*Reports and Memoranda No. 3169\**

*August, 1956*

---

*Summary.*—The paper describes an investigation of the effect of structural damping in the torsion mode on wing flutter with the object of finding circumstances in which damping reduces the flutter speed. The drop in flutter speed can be considerable (25 per cent) and extend to very large values of structural damping. The effect is most apparent when the relative density (wing to air) is high, and when the wing bending mode involves a relatively large aerodynamic stiffness.

The rate of decrease of flutter speed with damping is small, and for the amounts of damping normally encountered in practice the effect is unlikely to be important. Possible practical cases are, however, part-full under-wing fuel tanks, which can supply high structural damping, and large tailplane amplitudes in the wing torsion mode, which can supply considerable aerodynamic damping; in both cases the effect could be appreciably adverse.

---

1. *Introduction.*—It is well known that if a small amount of structural damping is added to one degree of freedom in a binary-flutter problem the critical flutter speed can be reduced thereby. If control-surface flutter is to be prevented by hydraulic damping rather than mass-balance, for example, the curve of flutter speed against damping often falls for a little way. The examples considered later are rather more academic than this, since they are concerned with flexure-torsion wing flutter where the deliberate variation of structural damping is not normally possible, but they are noteworthy because a very large value of the structural damping is necessary before the flutter speed starts to increase. Certain cases where the effect might be important are discussed in the conclusions to the paper; they include an under-wing fuel tank partly full, and the effect of tail aerodynamic damping on a wing mode.

The first example was discovered during the routine solution by means of the Royal Aircraft Establishment Flutter Simulator of a wing flutter problem on a particular aircraft. When operating the simulator it is often desirable to reduce the amplitude of the motion, and a common way of doing this is to introduce a large amount of structural damping into the direct term of one of the essential degrees of freedom. In the present case this was found to increase the oscillations, and subsequent investigation showed that the same effect occurred even in a binary calculation. In a larger calculation, such as the quinary from which this binary was taken, structural damping in one degree of freedom could have an adverse effect merely by suppressing a stabilizing degree of freedom; this explanation cannot hold for a binary in which each degree of freedom is essential to the flutter. The present paper describes this binary calculation, which was carried out on a desk machine, and some later investigations made to decide how general the effect is likely to be as well as to consider its characteristics in more detail. A criterion for the fall of flutter speed with damping is discussed and an example shows that the effect can occur in the bending mode as well as the torsion mode.

---

\* R.A.E. Report Structures 212, received 27th December, 1956.

2. *The Binary Calculations for Wing Flutter.*—The calculations discussed in this and the next Section are primarily of academic interest. The results have had no repercussions on the aircraft to which they relate, because a serious drop in flutter speed with structural damping only occurs at high altitude (the specific calculations quoted relate to 55,000 ft) where the flutter speed is in any case far outside the capabilities of the aircraft. This need not always be so, however, as an increase in altitude differs in only a minor way (due to the aerodynamic inertias) from an overall increase in the wing density and in this case the wing density was not particularly high. It is shown in a later section (Section 4.2) that the flutter speed of a *Meteor* wing carrying a heavy mass falls rapidly with structural damping at quite moderate heights, so that the problem itself may have practical importance in other examples.

In this case it is only in the torsional mode that an increase in structural damping causes a reduction in the flutter speed, so the direct torsional damping of the structure is the parameter which has been varied in the calculations. The more general implications are discussed in Section 6, but it is worth noting that the torsional mode, which involves shear distortion, is likely to contain more structural damping than the bending mode. Although the phenomenon was first noticed, in this particular case, on the R.A.E. Flutter Simulator during a larger calculation, the binaries of this Section were solved on a desk machine for greater precision.

The wing concerned possesses moderate sweepback and carries no large concentrated masses. The modes are antisymmetric resonance modes and possess no unusual features; the nodal line in the torsion mode runs along the span at roughly the half-chord location.

2.1. *The Flutter Coefficients.*—The equations of motion at the flutter speed, appropriate to the generalised co-ordinates  $q_1$  for bending and  $q_2$  for torsion, are

$$\begin{bmatrix} 4400\lambda^2 + 210\lambda + 493 + 941y, & 17\lambda^2 - 21\lambda + 389 \\ 84\lambda^2 - 26\lambda - 826, & 718\lambda^2 + 86\lambda - 432 + 1100y \end{bmatrix} \begin{bmatrix} q_1 \\ q_2 \end{bmatrix} = 0. \quad \dots \quad (1)$$

Here  $\lambda^2 = -v^2$

$v$  is the frequency parameter  $\omega c_r/V$  based on a reference chord  $c_r$ ,

$\omega$  is the flutter frequency

$V$  is the flutter speed

$y = (V_0/V)^2 = (1/v)^2$

$V_0$  is a reference speed.

This is the standard way of writing the flutter equations in Great Britain, and assumes that the aerodynamic coefficients are independent of frequency parameter. This assumption does not lead to serious error as a rule, particularly when the aspect ratio is not large<sup>1</sup>. Equation (1) is written in the form suitable for solution on a desk machine, for which purpose the determinant of the second-order matrix is equated to zero, but the coefficients have been derived from the values prepared for the simulator. To change the coefficients from one form of the equations to another<sup>2</sup> (*i.e.*, from being suitable to the simulator to being suitable for desk solution, and *vice versa*) is a simple matter and in the present case only involved a correction for the time constant of  $\frac{1}{2}$  used in degree of freedom (1). The solution of equation (1) is usually carried out for  $y$  and  $\lambda$  only;  $y$  gives the flutter speed (it is inversely proportional to the square of the flutter speed) and  $\lambda$  gives the frequency parameter, from which, the flutter speed being known, the flutter frequency can be found.

It may be noted that each degree of freedom contains positive aerodynamic damping (+ 210 and + 86 units respectively) and that the cross-dampings are small. The direct aerodynamic stiffness for bending (+ 493 units) is positive and of reasonable size, as befits the bending mode of a swept-back wing, while that for torsion (− 432 units) is typically negative. The direct inertias (aerodynamic and structural) are large and positive (+ 4400 and + 718 units) and so



where  $a_{22}$  is the torsional inertia coefficient (718 units) and  $e_{22}$  is the elastic torsional stiffness coefficient (1100 units). In this example  $(d_{22})_{crit}$  has the value 1780 units. The advantage of relating the damping to critical damping is that it gives a measure of the rate of decay of the motion at zero air speed, as determined in a ground resonance test. Specifically

$$\frac{d_{22}}{(d_{22})_{crit}} = \frac{1}{2\pi} (\text{logarithmic decrement}) \dots \dots \dots (7)$$

If desired, the equivalent phase lag (hysteresis) damping can be calculated in any particular case, the relation depending on the frequency. Hysteresis damping is usually written in terms of the coefficient  $g$  (in this case  $g_{22}$ ) by replacing the pure stiffness term  $e_{22}$  by the term  $e_{22}(1 + ig_{22})$ . For this to be equivalent to the damping of equation (5), we must have

$$d_{22}\lambda\sqrt{y} = ie_{22}g_{22}y, \dots \dots \dots (8)$$

i.e.,

$$g_{22} = \frac{d_{22}}{e_{22}} \frac{\omega c_r}{V_0} \dots \dots \dots (9)$$

The aerodynamic damping,  $b_{22}$ , is of velocity type, so that at a given speed it is directly interchangeable with the structural damping  $d_{22}$ , but not, however, with  $g_{22}$ .

2.2. *Variation of Flutter Speed with Structural Damping.*—The change of flutter speed with fractions of critical damping in the torsion mode is given in Table 1, and shown also in Fig. 1.

TABLE 1

$d_{22}$ (per cent crit)	$v$ (per cent)	$x = -\lambda^2 = \nu^2$	$\frac{\omega c_r}{V_0}$	$g_{22}$
0	100	0.53	0.70	0
10	91	0.49	0.61	0.099
30	81	0.53	0.57	0.277
60	79	0.52	0.55	0.534
100	81	0.49	0.54	0.874
200	96	0.37	0.56	1.81

It will be seen that the flutter speed falls immediately on introducing the structural damping, in contrast to the case of the *Meteor* with tip mass discussed later, and reaches a minimum over 20 per cent lower than the original speed. Even more surprising is the scale of the structural damping involved.

It is indeed a remarkable fact that the wing flutter speed with 100 per cent critical damping in the torsion mode should be 19 per cent less than for the undamped wing. This means that the torsional oscillations of the wing change from being dead beat at zero speed to a state of growing violently with time at a  $v$  of 100 per cent, by which time the wing without structural damping has only just returned to its initial condition of undamped sinusoidal motion.

To examine this fact in more detail, the roots of equation (1) were obtained at speeds below the flutter speed with  $d_{22}$  having the two values of zero and critical damping. The solutions are given in Figs. 2 and 3. It can be seen from Fig. 2 (which shows the results for no structural damping) that one root becomes progressively more heavily damped while the other shows a maximum damping at about 75 per cent of the flutter speed, after which the rate of decay falls steeply. This is quite a typical result in itself, but what is less usual is that the higher-frequency root, which starts as the pure torsion mode at zero speed, is the one which becomes progressively more damped, whereas the lower frequency root leads to flutter. With critical damping in the torsional mode there is no speed for which the torsional root (*i.e.*, the root which defines pure torsion at zero speed) is oscillatory; the bending root again leads to flutter after reaching a

maximum rate of decay at about 60 per cent. of the flutter speed. It is shown in a later example that when the torsional root leads to flutter with zero structural damping in its mode, there is a change over and the flexural mode leads to flutter after a relatively small amount of structural damping has been introduced.

3. *Analysis of the Forces in the Binary of Section 2.*—The results given in the previous Section were sufficiently surprising to the authors for an investigation of the balance of forces to be undertaken. It is clear that the amount of energy extracted from the air stream must increase considerably as the structural damping in the torsion mode is increased ; the mechanism is of some interest.

3.1. *The Amplitude Ratio of the Two Co-ordinates at Flutter.*—In Fig. 4 the generalised co-ordinate  $q_2$  is represented by a unit vector at the critical flutter condition. The corresponding vectors  $q_1$  are drawn on the same diagram for several solutions of the flutter equations with different values of the torsional structural damping. The phase difference between the two co-ordinates is initially very small (*i.e.*, when  $d_{22} = 0$ ) but becomes steadily larger as  $d_{22}$  is increased. This change is to be expected, since only by making the phase angle more favourable to flutter can more energy be extracted from the air stream. It is to be noted that the phase angle is initially very small and it is probably only in such circumstances that the flutter speed actually falls when structural damping is added. The modulus of  $q_1$  also increases with torsional damping so that the motion as seen by an observer would change from being primarily torsional in character to being primarily bending in character.

3.2. *The Balance of Forces at the Flutter Speed.*—The balance of forces is indicated by the vector diagrams of Figs. 5 and 6. Fig. 5 refers to the second Lagrangian equation, *i.e.*, the equation of work done in a small torsional displacement,

$$(84\lambda^2 - 26\lambda - 826)q_1 + (718\lambda^2 + 86\lambda - 432 + 1100y + d_{22}\lambda\sqrt{y})q_2 = 0 \quad \dots \quad (10)$$

The diagrams are drawn from the equation in this non-dimensional form, but for an equivalent displacement of  $q_2$  in each case. To do this the quantity  $1100yq_2$ , which is proportional to the strain energy in the torsional mode and therefore to the torsional displacement, is equated to unity in each case. It is because the flutter equations, *e.g.*, equation (10), are divided through by  $V^2$  that the speed factor  $y$  appears in this relation and  $q_2$  itself is not constant throughout Fig. 5 ; this method adopted in drawing the diagrams of Fig. 5 retains the non-dimensional form of the equation but cancels the misleading effect of the division by  $V^2$ .

The vector diagram for  $d_{22} = 0$  is shown in Fig. 5a. The length  $OA$  represents the term in phase with  $q_2$  from the second bracket of equation (10). Thus

$$OA = (718\lambda^2 - 432 + 1100y)/1100y = 0.32, \quad \dots \quad (11)$$

since  $\lambda^2 = -0.53$  (*see* Table 1) and  $y = 1.085$ . The vector  $AB$  represents the damping term from the same bracket acting at 90 deg phase ; in this case since  $d_{22} = 0$  the term is entirely aerodynamic ( $= 86\lambda/1100y$ ). The vector  $OB$  represents the forces acting in the co-ordinate  $q_2$  due to the motion of  $q_2$  : the vector  $BO$  must therefore, for balance, represent the forces acting in the co-ordinate  $q_2$  due to the motion of  $q_1$ . This is made up of the component  $BC$  in phase with  $q_1$  and the small component  $CO$  at 90 deg phase. The value of  $BC$  is given by

$$\vec{BC} = (84\lambda^2 - 826)\vec{q}_1, \quad \dots \quad (12)$$

where  $\lambda^2 = -0.53$  as before and  $\vec{q}_1$  has the appropriate value given by Fig. 4.

Figs. 5b, 5c and 5d show the corresponding diagrams with progressively increasing values of  $d_{22}$ , but although in Fig. 5d the value of  $d_{22}$  much exceeds critical damping for the torsion mode the flutter speed is still rather less than in Fig. 5a. In all these examples the vector  $OA$  is considerably greater than in Fig. 5a, partly because of the larger values of  $y$  (lower flutter speeds), particularly in Figs. 5b and 5c, and partly because of the less negative values of  $\lambda^2$  (*see* Table 1) particularly in Fig. 5d. The direct damping vector ( $AB$ ) increases rapidly with  $d_{22}$  to a value of

nearly fifty times that of Fig. 5a by Fig. 5d. In the meanwhile, however, the vector  $q_1$  has increased in magnitude and phase so that  $BC$  again almost closes the diagram in each case. It may be noted that the vector  $OA$  is positive throughout Fig. 5 because the flutter frequency is lower than the frequency of mode two taken alone, at the appropriate airspeed.

Fig. 6 gives the corresponding diagram for the first equation

$$(4400\lambda^2 + 210\lambda + 493 + 941y)q_1 + (17\lambda^2 - 21\lambda + 389)q_2 = 0 \quad \dots \quad (13)$$

in which the bending displacement, proportional to  $941yq_1$ , has been made unity in each case. In these diagrams the vector  $OA$ , which again represents the direct in-phase term, is negative, e.g.,

$$OA = (4400\lambda^2 + 493 + 941y)/941y = -0.54 \quad \dots \quad (14)$$

for the condition  $d_{22} = 0$  in Fig. 6a. This is so because the frequency of mode (1) taken alone, at the appropriate air speed, is below the flutter frequency. It is necessary that this mode should approach more and more closely to a resonant condition as the magnitude of  $q_2$  shrinks with increasing  $d_{22}$ , since otherwise the distance  $BO$  could not be spanned by the coupling terms. That this does in fact happen is indicated clearly by Fig. 6 as the point  $A$  steadily approaches the origin.

4. Survey of some Recent Binary Wing Flutter Calculations.—4.1. Analysis of the Results.—Following the detailed investigation described above, a survey was carried out of a number of binary wing flutter calculations to decide how common is the effect of reducing flutter speed with increasing torsional damping. This survey indicated that the effect is always much more pronounced at high altitude than at low, and that the occasions on which it is important at low altitude are very few. This clearly suggests that it is the initial values of the damping coefficients which have most significance in deciding whether or not the effect will exist. In particular the damping in the bending mode might be expected to be the more important since for quite large values of the structural damping in torsion (see Fig. 1 for example) the flutter speed is still falling.

Because of the importance of the aerodynamic dampings, the results of the survey are given in Table 2 together with the appropriate damping coefficients.

TABLE 2

	Type of aircraft	Height (ft)	$\frac{b_{11}v}{2\sqrt{(a_{11}e_{11})}}$	$\frac{b_{22}v}{2\sqrt{(a_{22}e_{22})}}$	$\frac{\delta v}{v}$ per 10% $d_{22}$
1	Bomber type, moderate sweepback, aspect ratio 5 to 6.	40,000	0.0498	0.123	-0.09
2		sea level	0.938	0.102	+0.283
3		40,000	0.418	0.0454	0.273
3a		sea level	0.443	0.193	0.01
		40,000	0.651	0.492	0.258
		sea level	0.239	0.180	0.0266
4	Delta aircraft, fighter size	sea level	0.789	0.292	0.072
		40,000	0.340	0.126	+0.029
5		sea level	0.164	0.152	-0.0064
		40,000	0.0797	0.0741	-0.0687
6	Straight wing fighter	sea level	0.0939	0.0994	+0.014
		40,000	0.0469	0.0497	-0.0536
7		sea level	0.101	0.0966	+0.192
7a	Unswapt bomber; high aspect ratio.	40,000	0.0464	0.0442	0.0279
		sea level	0.0344	0.0411	+0.0115
8	Hypothetical	40,000	0.0167	0.0199	-0.0741
		sea level	0.305	0.191	+0.083
9		40,000	0.149	0.0937	+0.096
			0.00981	0.0944	-0.058

In the first column each different number refers to a different aircraft ; 3a and 7a refer to the same aircraft as 3 and 7 respectively, but in 3a the calculation is antisymmetric instead of symmetric, and in 7a the calculation covers a different loading condition. The fourth and fifth columns give the aerodynamic damping in the bending and torsional modes respectively. The damping is expressed as a fraction of critical damping at the flutter speed, and the large variation in this quantity is of some interest in itself. In those cases where the dampings are large, such as 2 and 4, a considerable phase difference will already be present at flutter so that little increase can be expected with the addition of structural damping, and hence the flutter speed must increase. The change in flutter speed caused by increasing  $\bar{d}_{22}$  from zero to a value of 10 per cent critical damping is given as a fraction of the initial flutter speed in column 6. It can be seen that the only examples of a drop in flutter speed (with the exception of 5, in which a very small drop occurs at sea level, and 9 in which the height datum is arbitrary) occur at 40,000 ft. This suggests that the effect is unlikely to have great practical significance, but there is one exception, not given in Table 2, and that is the *Meteor* with a heavy wing tip mass which is treated separately in the next Section. Aircraft 7 and 8 of Table 2 both carry tip masses, and aircraft 4 carries a heavy mass in the outer half of the wing.

The change in flutter speed (column 6 of Table 2) is plotted in Fig. 7 against the damping values given by columns 4 and 5. There is clearly a general tendency for the low damping values to give the negative and low positive values of  $\delta v/v$  but the scatter is considerable. In view of this an attempt has been made to deduce a theoretical expression for the condition that the flutter speed will initially fall with the addition of structural damping  $\bar{d}_{22}$ . To simplify the analysis, the assumption has been made that the only coupling terms are the aerodynamic cross-stiffnesses. This is justified if the coefficients are similar to those of equation (1), but there are many exceptions to this, in particular any calculations in which the modes are far from normal (*e.g.*, assumed arbitrary modes), and also those cases in which the first mode involves no aerodynamic incidence change\*.

With this approximation the condition for  $\partial V/\partial \bar{d}_{22}$  to be negative at  $\bar{d}_{22} = 0$  is that  $t_1$  should be negative, where

$$t_1 = y\{b_{11}b_{22}(a_{11}e_{22} + a_{22}e_{11}) + 2a_{11}b_{22}^2e_{11}\} + b_{11}b_{22}(a_{11}c_{22} + a_{22}c_{11}) + 2a_{11}b_{22}^2c_{11} + c_{12}c_{21} \left( a_{11}^2 \frac{b_{22}}{b_{11}} - a_{22}^2 \frac{b_{11}}{b_{22}} \right). \quad (15)$$

The standard notation is used, so that  $a_{rs}$  is a typical inertia coefficient,  $b_{rs}$  a typical aerodynamic damping coefficient,  $c_{rs}$  a typical aerodynamic stiffness coefficient, and  $e_{rs}$  a typical structural stiffness coefficient.

The analysis leading to equation (15) is given in the Appendix, as is the extended form of  $t_1$  when  $b_{21}$  is not zero.

The term involving  $y$  in  $t_1$  is positive as long as the direct aerodynamic damping coefficients are positive, which they always are in practice at subsonic speeds. The term independent of  $y$  in  $t_1$  involves the aerodynamic stiffness coefficients (the  $c$ 's) and can therefore be negative, but it will be noticed that the first part of this term is identical with the term in  $y$  except that the aerodynamic stiffnesses replace the corresponding elastic stiffnesses. It follows that if the critical flutter speed is below the divergence speeds both of degree of freedom 1 by itself and of degree of freedom 2 by itself, then that part of  $t_1$  which excludes the coupling coefficients must be positive. Accordingly  $t_1$  can only be negative if

$$\frac{a_{11}}{b_{11}} > \frac{a_{22}}{b_{22}}, \quad \dots \quad (16)$$

since the product  $c_{12}c_{21}$  must be negative for a real flutter speed to exist.

---

\* For example, the flutter of an unswept wing with the flexural and inertial axes coincident at the half-chord ; in this case  $a_{21}$  and  $c_{21}$  will be zero (or nearly so) but  $b_{21}$  will be relatively large and negative. An extension covering this case is given in the Appendix.



From the form of (15) and (16) we may summarise the rules for an initial reduction in flutter speed with structural damping as :

- (1) The product  $c_{12}c_{21}$  should be negative and large compared with the products of the direct dampings,  $b_{11}^2$ ,  $b_{11}b_{22}$  and  $b_{22}^2$ \*
- (2) If (1) is true, then the flutter speed will drop with increasing  $d_{22}$  if

$$\frac{a_{11}}{b_{11}} \gg \frac{a_{22}}{b_{22}}$$

and the flutter speed will drop with increasing  $d_{11}$  if

$$\frac{a_{22}}{b_{22}} \gg \frac{a_{11}}{b_{11}}$$

The second part of (2) follows by interchanging the suffixes in the expression for  $t_1$ . The first rule is quite rough and assumes that the coefficients have been scaled to the same order of magnitude in each degree of freedom, and that the flutter-speed parameter is of the order of unity. The effect is, however, fairly clear, as shown by Fig. 8 in which  $\delta v/v$  is plotted against the quantity  $(-c_{12}c_{21}/b_{11}b_{22})$ ; the points follow the dotted curve reasonably well, and what scatter there is arised mainly from the different values of  $(a_{11}/b_{11} - a_{22}/b_{22})$ .

4.2. *The Meteor with Tip Mass.*—This case is especially interesting because of the very large value of the quantity  $(-c_{12}c_{21}/b_{11}b_{22})$ , which is, in fact, 139 units at 15,000 ft, the altitude at which most of the calculations have been carried out. This means that the term in  $c_{12}c_{21}$  in the expression (15) for  $t_1$  plays a dominating part. The coefficients at 15,000 ft are given by†

$$\Delta \equiv \begin{vmatrix} 1032\lambda^2 + 158\lambda + 104 + 1110y, & -100\lambda - 3544 \\ 8\lambda + 1110, & 616\lambda^2 + 90\lambda - 80 + 2660y \end{vmatrix} \dots \quad (17)$$

The last term of the expression for  $t_1$  is

$$t_2 = c_{12}c_{21} \left( a_{11}^2 \frac{b_{22}}{b_{11}} - a_{22}^2 \frac{b_{11}}{b_{22}} \right) \dots \dots \dots \quad (18)$$

$$= -3.934(0.6067 - 0.6662) \times 10^{12} \dots \dots \dots \quad (19)$$

using the coefficients of equation (17). The quantity  $t_2$  is clearly positive so that the flutter speed increases with the addition of  $d_{22}$ . Unless the speed is changing very rapidly, however, an increase in  $d_{22}$  will have the same general effect as an increase in  $b_{22}$  at a slightly different rate. Now, because of the small difference in equation (19), an increase in  $b_{22}$  soon makes  $t_2$  negative, and because  $t_1$  in this example depends principally on the value of  $t_2$  it follows that  $t_1$  also soon becomes negative. It is therefore to be expected that although the flutter speed increases with  $d_{22}$  initially it will soon start to fall as the controlling term  $t_2$  effectively becomes negative on allowing for  $d_{22}$ . The graph of  $V$  against  $d_{22}$  therefore shows an initial increase followed by a prolonged decrease, as shown in Fig. 9, with a minimum flutter speed about 75 per cent of the basic value.

\* In wing flutter, the equivalent air-speed at the critical flutter condition does not vary much with height, and this speed (rather than the true speed) is obtained if the height variation is effected by multiplying the  $b$ 's by  $\sqrt{\sigma}$  and the  $\bar{a}$ 's by  $\sigma$ ; where  $\sigma$  is the air density ratio and  $\bar{a}$  the aerodynamic inertia (the change in the  $\bar{a}$ 's is often neglected). In applying rule (1), therefore,  $b\sqrt{\sigma}$  should be used rather than  $b$  itself if the altitude is other than sea level. This has been done in the text and in plotting Figs. 7 and 8.

† These coefficients correspond to  $-c_{12}c_{21}/b_{11}b_{22} = 277$ , because they have been corrected for time constants. Strictly, however, this quantity should be compared on the basis of coefficients scaled to give unit critical speed ( $y = 1$ ) and frequency ( $\lambda = i$ ). If this is done the ratio drops to 69. For the purpose of applying the rough rule of Section 4.1 it is good enough to take the coefficients directly as scaled for the simulator since the mean frequency (and the flutter speed) should be not very far from unity; this gave 139 units as quoted in the text.

On the same Figure is plotted the effect of an increase in  $d_{11}$ . In this case the flutter speed falls immediately with increase in damping, as would be expected from the application of the rules given in the last Section, but the maximum drop in flutter speed is less with  $d_{11}$  than with  $d_{22}$ , the minimum speed being about 85 per cent of the value with no damping. By the time  $d_{11}$  has been increased to 2.04 times critical damping, the flutter speed has returned to its initial value, and thereafter rises steadily. For comparison the flutter speed is below its initial value when  $d_{22}$  lies between 0.054 and 3.66 times critical damping.

Although a large drop in flutter speed can be obtained by the introduction of structural damping either in mode 1 or in mode 2, the form of equation (15) shows that the two effects are not additive. The result of adding a constant proportion of critical damping in each degree of freedom is shown in Fig. 9, and it can be seen that the increase of flutter speed is quite steady.

The amplitude ratio ( $q_1/q_2$ ) is plotted in Fig. 10 (and the amplitude ratio  $q_2/q_1$  in Fig. 11) for those values of  $d_{22}$  which give the same flutter speed as when  $d_{22} = 0$ . The effect is much the same as for the example of Section 3, the initial phase difference between  $-q_1$  and  $q_2$  is about 10 deg and by the time  $d_{22}$  has increased to 3.66 times critical damping this phase angle has reached about 80 deg. The sign of the co-ordinate  $q_1$  relative to  $q_2$  is, of course, just a matter of the initial choice, and in the present example the choice made was clearly the opposite of that made for the example of Sections 2 and 3 (compare the sign of the aerodynamic cross-stiffnesses in equations 1 and 17). At the same time as the phase angle is increasing through 70 deg, the amplitude ratio increases about 16 times.

The converse, for increasing  $d_{11}$ , is shown in Fig. 11. Again the phase difference increases, to about 75 deg by the time the flutter speed has returned to its original value. At the same time the amplitude of the undamped mode ( $q_2$  in this case) increases several times. The increase is not so marked as when  $d_{22}$  is increased, being about 5 times compared with 16. Another interesting effect is on the flutter frequency; in the examples where  $d_{22}$  is increased this frequency falls steadily, but when  $d_{11}$  is increased the flutter frequency increases; in general it appears that the flutter frequency tends towards the natural frequency of the mode whose amplitude is increasing.

As in the example of Section 2 the complex latent roots of the binary calculation have been evaluated at speeds below the critical flutter speed for  $d_{11} = 0$  and  $d_{22} = 0, 0.054$  and  $3.66$  times critical damping respectively; these three conditions all give the same flutter speed. When  $d_{22} = 0$  the torsion mode leads to flutter whilst the bending mode becomes progressively more damped, but between  $d_{22} = 0$  and  $d_{22} = 0.054$  times critical damping the two change over as shown in Fig. 12b. For some intermediate damping ratio the behaviour would be such as to render flight flutter tests difficult to analyse, because of the rapid change in frequency of the two roots, and the sudden drop in damping to the flutter condition. For the largest value of  $d_{22}$ , as shown in Fig. 12c the torsional root is dead beat all the way.

5. *Binary Investigations of a Hypothetical Wing.*—In an attempt to understand what type of normal modes give rise to a form of flutter in which the critical speed falls with structural damping in one of the modes, some calculations were made in the reverse direction starting with a range of coefficients known to cause the required effect, and, assuming standard derivatives, working back to the modes. A certain amount of trial and error was involved, and the resulting modes for a rectangular wing do not look very plausible (see Fig. 13). The flutter equations are

$$\begin{bmatrix} 4000\lambda^2 + 26\lambda + 37 + 1000y, & 110\lambda + 183 \\ -84\lambda - 225, & 250\lambda^2 + 63\lambda - 313 + 1000y \end{bmatrix} \begin{bmatrix} q_1 \\ q_2 \end{bmatrix} = 0$$

and the resulting fall in flutter speed with  $d_{22}$  is indicated in Fig. 14.

If the flexural and inertial axes coincide for an unswept wing, then  $c_{21}$  is nearly zero but  $b_{21}$  will provide sufficient coupling to promote flutter if the combined axis is sufficiently far aft of the aerodynamic centre. The expression corresponding to  $t_1$  for this case is given in the Appendix and it is only for most unlikely conditions that the value becomes negative. A particular example of an unswept wing with an extreme frequency ratio (favourable to negative  $t_1$ ) has been worked out on the assumption of pure bending for mode one and pure torsion for mode two, but the flutter speed increases with  $d_{22}$  at all practical heights.

It is concluded from these investigations that the conditions in which the flutter speed may fall on the addition of structural damping are :

- (1) The relative density (wing to air) must be high.
- (2) The wing normal modes must involve coupled flexure and torsion\*, either
  - (i) through sweepback
  - (ii) through a wide separation between the flexural and inertial axes
  - (iii) through the presence of large concentrated masses with offset c.g.s.

All the examples of Table 2 in which  $\delta v/v$  is negative satisfy both these conditions, although it is to be noted that deltas must be classed as swept-back aircraft for this purpose.

6. *Conclusions.*—The results quoted in the present paper show that :

- (1) The binary wing flutter speed may fall on the addition of structural damping in either the torsional mode or the bending mode, but more often in the torsional mode.
- (2) The effect, if it occurs at all, gets worse with height, and often only takes effect at heights for which wing flutter presents no problem.
- (3) The drop in flutter speed may continue to very high values of the damping, and in some cases more than three times critical damping is necessary to raise the flutter speed above its initial value.
- (4) The drop in flutter speed for practical values of purely structural damping is small.
- (5) If damping is added in the same proportion in each mode the flutter speed always increases.

It can be concluded that in a routine wing flutter investigation the effect of structural damping is unlikely to be serious, but there are some circumstances in which damping is neglected, because it is thought to be beneficial, that could be dangerous. An example is that of a wing carrying under-wing fuel tanks partly full. It is usually considered that for the first few cycles of a flutter oscillation the damping effect of the fluid is small, and this is regarded as the dangerous period. When turbulence is set up in the fluid after a few cycles quite large values of structural damping in the wing torsion mode can occur (*see* Refs. 5 and 6, for example) ; if the flutter is of similar form to that of the *Meteor* with tip mass, for example, this, far from being beneficial, could have a serious adverse effect.

Another way in which one mode may have a large degree of damping associated with it is if the damping is aerodynamic, which would have the same basic effect as structural damping. Suppose the wing torsional frequency coincides with the tailplane bending resonance, for example. The tailplane effect might be neglected in flutter calculations by the argument that the wing torsion mode is supplied with a damper (aerodynamic in this case) which would be expected to be favourable ; again this could be dangerous.

Finally any device, or type of construction, intended to introduce a high degree of damping artificially as a wing flutter preventive must be carefully considered in relation to the particular application concerned.

---

\* The torsion to be understood in an aerodynamic sense.

Should a wing torsion mode be associated with very heavy structural damping in practice, it might lead to many difficulties which could be serious if the wing flutter was of the type discussed in the present paper. In the first place the mode would be very difficult to excite and measure accurately in a ground resonance test. Similarly any flight vibration work would be difficult to carry out on such a mode. This would not be so serious in one sense because the heavily damped mode is not the root which leads to flutter in the examples considered here, but on the other hand the bending mode might not be suspected as a possible dangerous mode. Added to these difficulties is the fact that the approach to flutter is rapid as shown in Figs. 3 and 12c, for example.

Mention should perhaps be made of the fact that in the present paper the effect of the damping forces on the mode itself has been neglected. Clearly this assumption might be seriously wrong when the damping reaches the order of critical damping, but unless there is a marked discontinuity in the distribution of damping the qualitative effects given in the paper are unlikely to be affected. In any case, whatever the source of the damping, values greater than about a quarter of critical are unlikely to be reached, but this amount can still give a substantial drop in flutter speed.

## LIST OF SYMBOLS

$q_r$	Generalized co-ordinate
$\nu$	Frequency parameter = $\omega c_r/V$ based on a reference chord $c_r$
$\lambda = i\nu$	
$\omega$	Flutter frequency
$V$	Flutter speed
$p_r$	Coefficient of $\lambda^n$ in the expansion of the flutter determinant ( <i>see</i> equation (2))
$T_3 =$	The 3rd test function
$l_1 =$	The coefficient of $2y$ in $T_3$
$l_2 =$	The constant term in $T_3$
$a_{rs} =$	$\hat{a}_{rs} + \bar{a}_{rs}$
$\hat{a}_{rs}$	Typical structural inertia coefficient
$\bar{a}_{rs}$	Typical aerodynamic inertia coefficient
$b_{rs}$	Typical aerodynamic damping coefficient
$c_{rs}$	Typical aerodynamic stiffness coefficient
$e_{rs}$	Typical structural stiffness coefficient
$d_{rs}$	Typical structural damping coefficient
$g$	Coefficient used in expressing hysteresis damping when the stiffness term $e$ is replaced by $e(1 + ig)$
$t_1$	$t_1 < 0$ gives the condition that $(\partial V/\partial d_{22})_{d_{22}=0} < 0$ , and is expressed in terms of $a, b, c, e$ and $y$ ( <i>see</i> Appendix and equation (15) in text)
$t_2$	Principal negative term in the expression $t_1$ ( <i>see</i> equation (16) in text)
$\sigma$	Air density ratio

## REFERENCES

- | <i>No.</i> | <i>Author</i>                    | <i>Title, etc.</i>   |
|------------|----------------------------------|--|
| 1          | I. T. Minhinnick .. ..           | A symposium on the flutter problem in aircraft design. Edited by H. Templeton and G. R. Brooke. Paper No. 4 : Aerodynamic derivatives. A.R.C. 16,081. May, 1953. |
| 2          | F. Smith and W. D. T. Hicks      | The R.A.E. electronic simulator for flutter investigations in six degrees of freedom or less. R. & M. 3101. September, 1954.                                     |
| 3          | R. A. Frazer and W. J. Duncan    | The flutter of aeroplane wings. R. & M. 1155. August, 1928.  |
| 4          | E. G. Broadbent .. ..            | <i>The Elementary Theory of Aero-elasticity.</i> Aircraft Engineering Bunhill Publications, Ltd., September, 1954.   |
| 5          | J. R. Reese .. ..                | Some effects of fluid in pylon mounted tanks on flutter. N.A.C.A. Research Memo. L35F10. T.I.B. 4634. July, 1955.  |
| 6          | E. Widmayer, Jr. and J. R. Reese | Moment of inertia and damping of fluid in tanks undergoing pitching oscillations. N.A.C.A. Research Memo. L53 EoLa. 1953.  |



If the total stiffness at the flutter speed ( $= c + ey$ ) is denoted by  $\sigma$ , equation (A.6) simplifies to

$$\frac{1}{b_{11}y^{1/2}} \frac{\partial T_3}{\partial d_{22}} = b_{11}b_{22}(a_{11}\sigma_{22} + a_{22}\sigma_{11}) + 2a_{11}b_{22}^2\sigma_{11} + c_{12}c_{21} \left( a_{11}^2 \frac{b_{22}}{b_{11}} - a_{22}^2 \frac{b_{11}}{b_{22}} \right). \quad \dots \quad \dots \quad (A.7)$$

If  $b_{21}$  is not zero, the additional term to be added to the right-hand side of equation (A.7) is

$$b_{21}c_{12} \left\{ \frac{a_{22}}{b_{22}} (a_{11}\sigma_{22} - a_{22}\sigma_{11}) + \frac{a_{11}a_{22}b_{21}c_{12}}{b_{11}b_{22}} \right\}. \quad \dots \quad \dots \quad \dots \quad \dots \quad (A.8)$$

In general  $c_{21}$  (equation (A.7)) and  $b_{21}$  (equation (A.8)) will be negative.



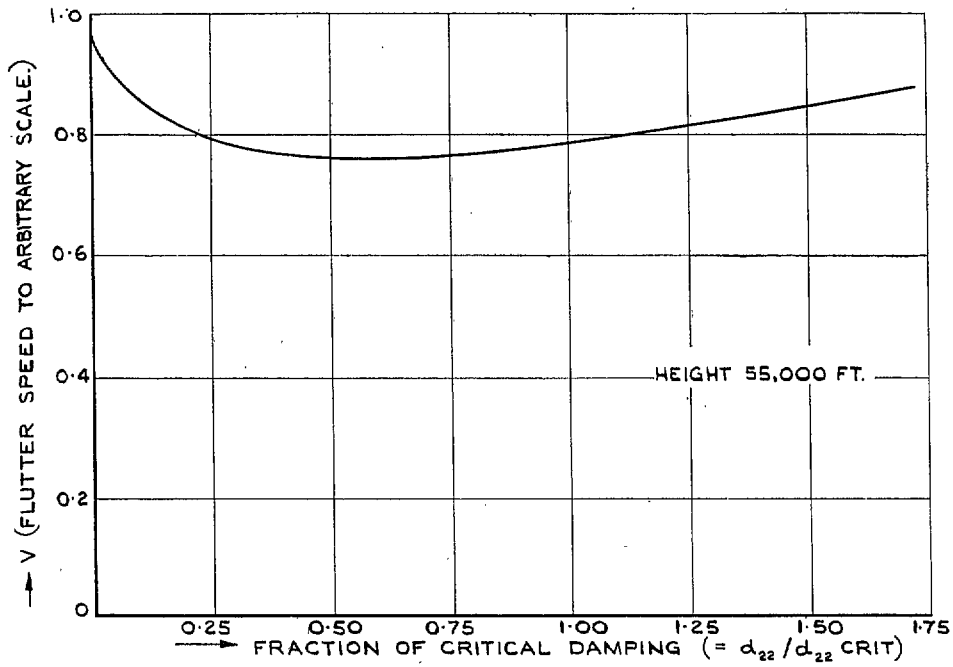


FIG. 1. An example of the variation of flutter speed with torsional damping.

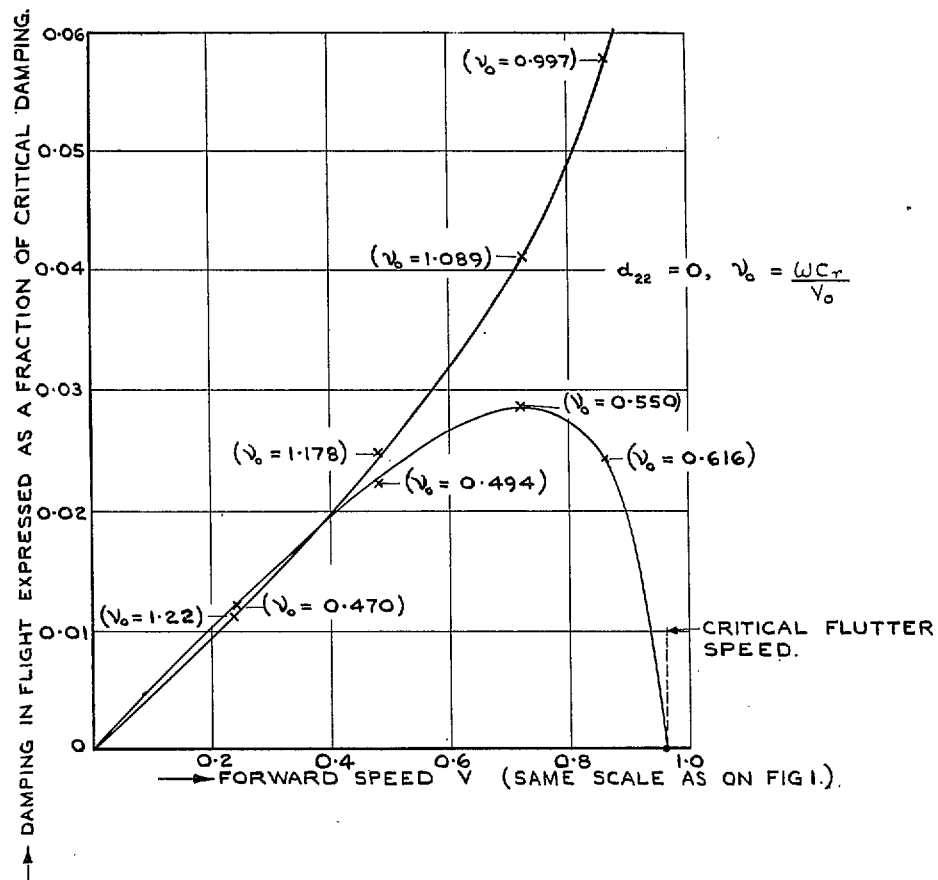


FIG. 2. The variation of flight damping with speed, with zero damping in the torsion mode.

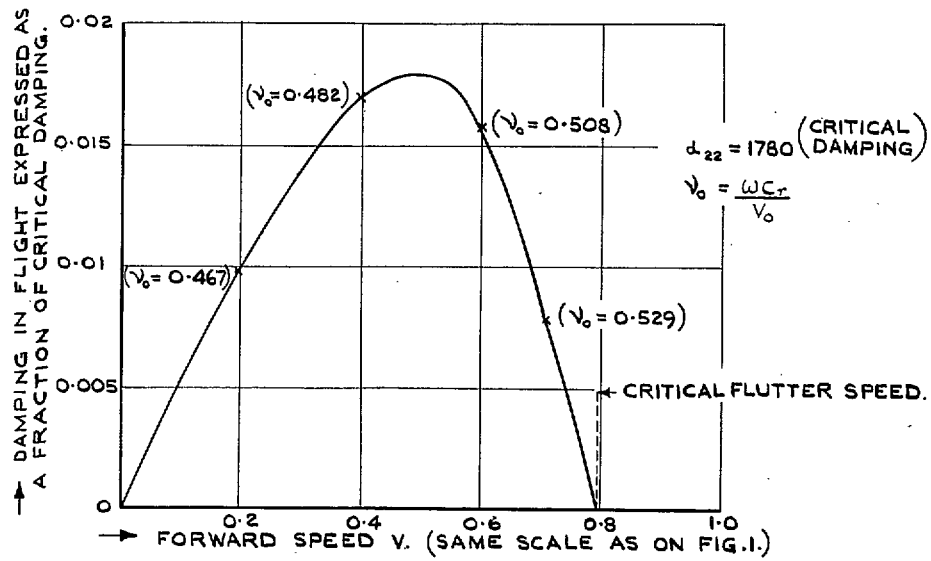


FIG. 3. The variation of flight damping with speed, with critical damping in the torsion mode.

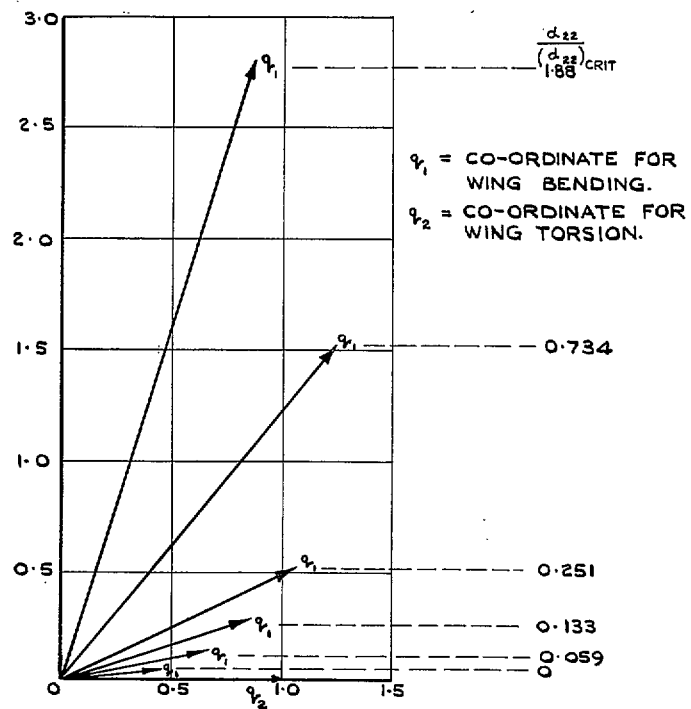
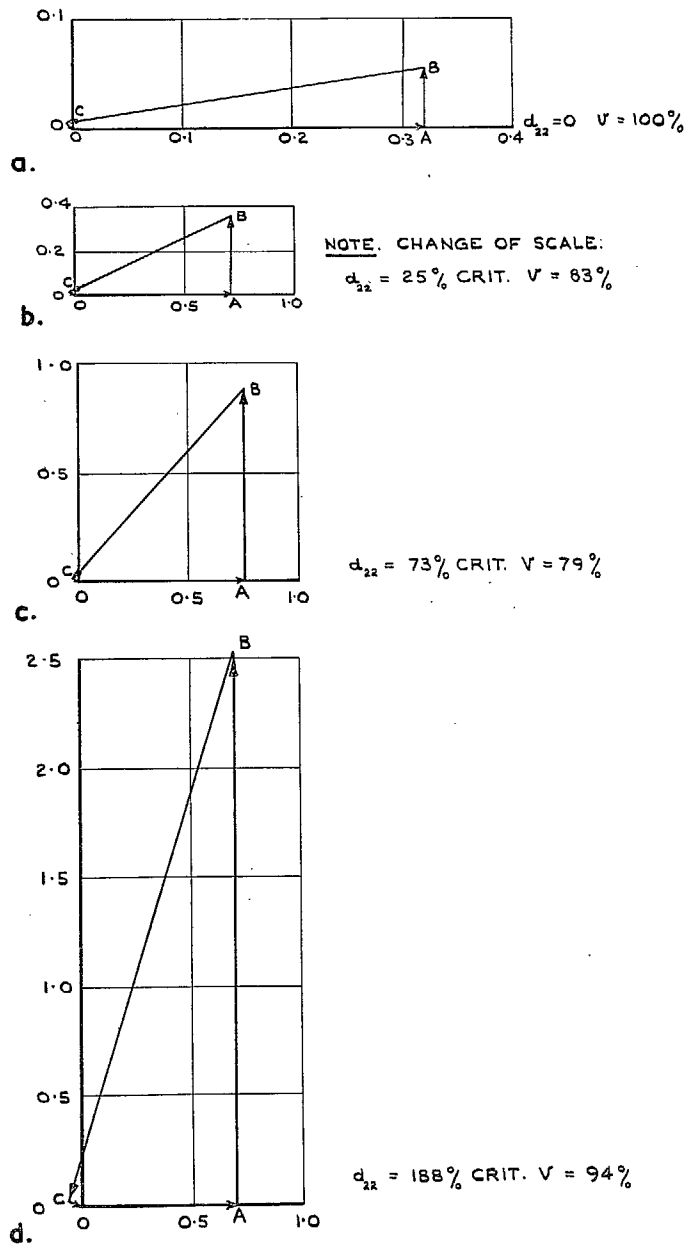
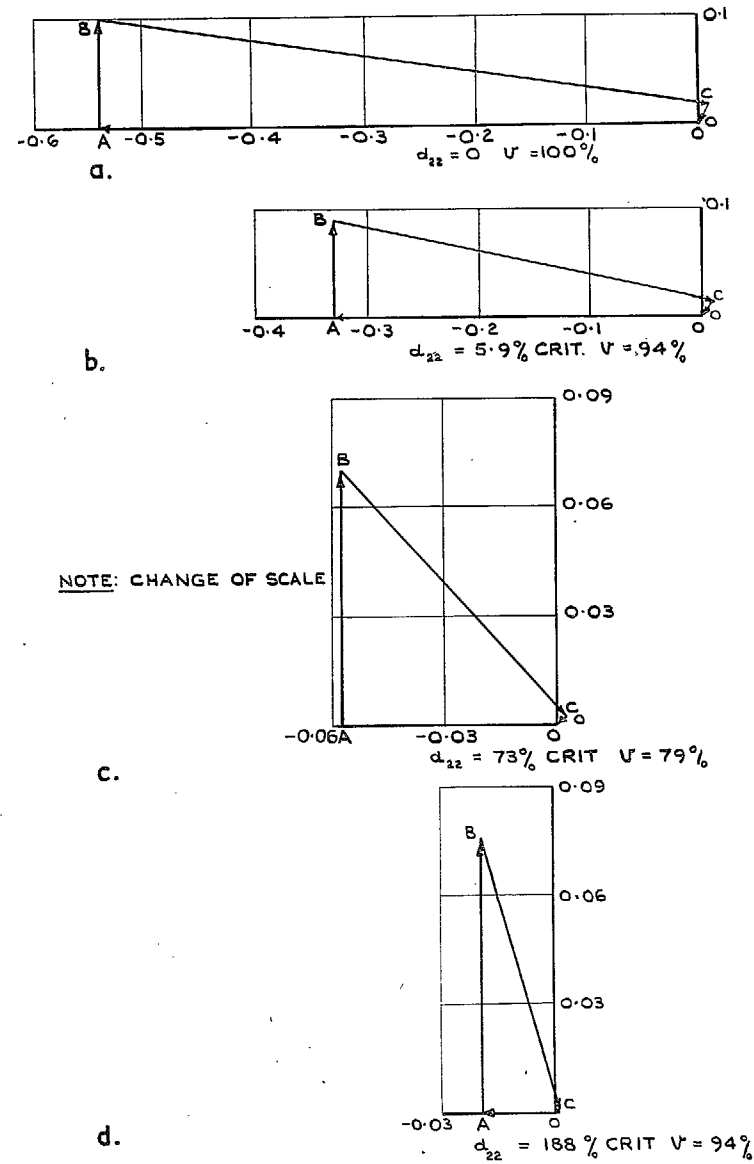


FIG. 4. Amplitude ratios for various values of torsional damping.



Figs. 5a to 5d. Force diagrams for different amounts of damping (Torsional equation).



Figs. 6a to 6d. Force diagrams for different amounts of damping (Bending equation).

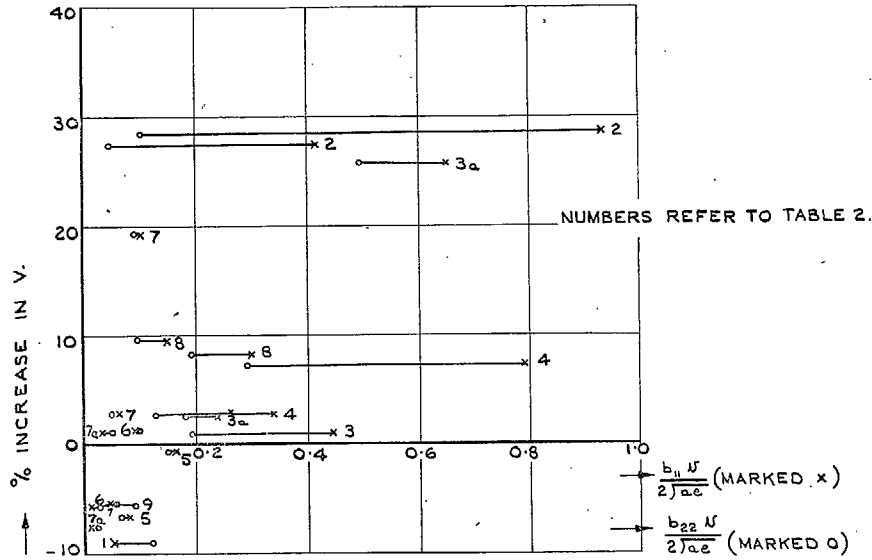


FIG. 7. Change in flutter speed for 10 per cent critical damping plotted against aerodynamic damping coefficients for several aircraft.

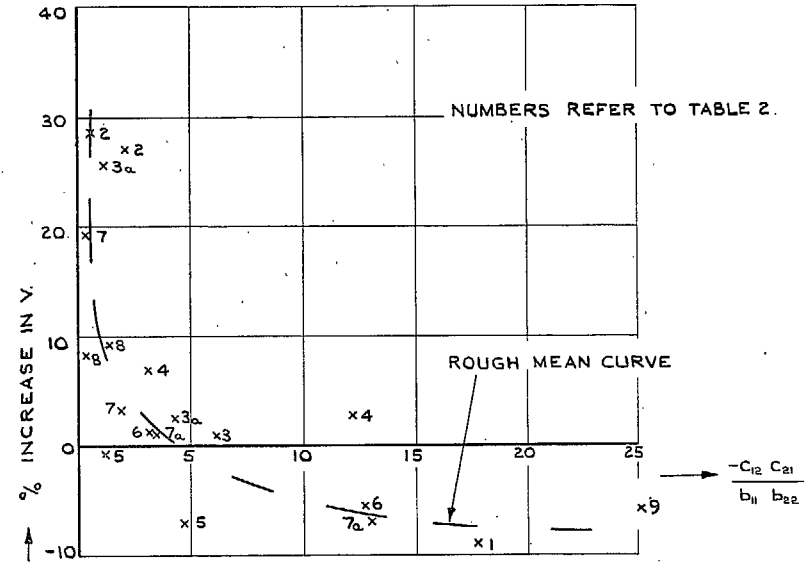


FIG. 8. Change in flutter speed for 10 per cent critical damping plotted against  $(-c_{12}c_{21}/b_{11}b_{22})$ .

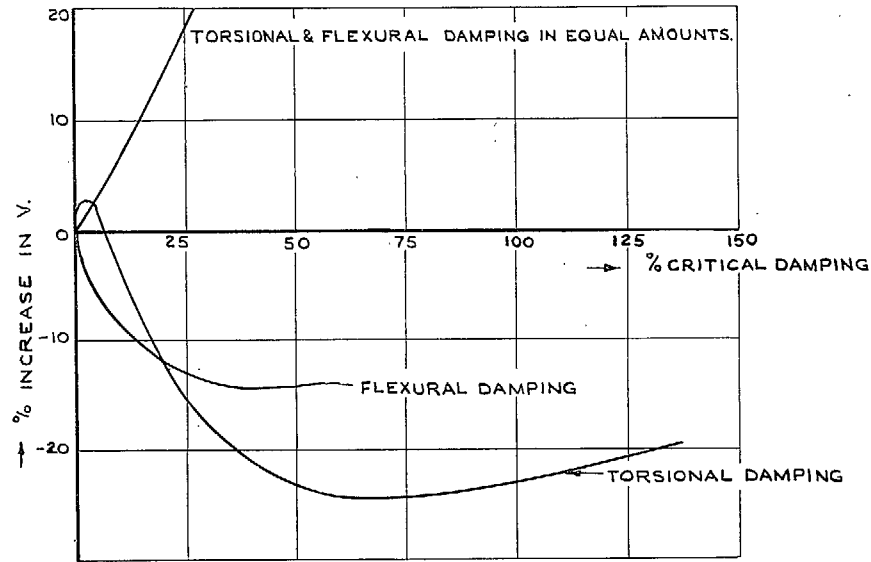


FIG. 9. Percentage increase in flutter speed for *Meteor* with tip mass plotted against structural damping.

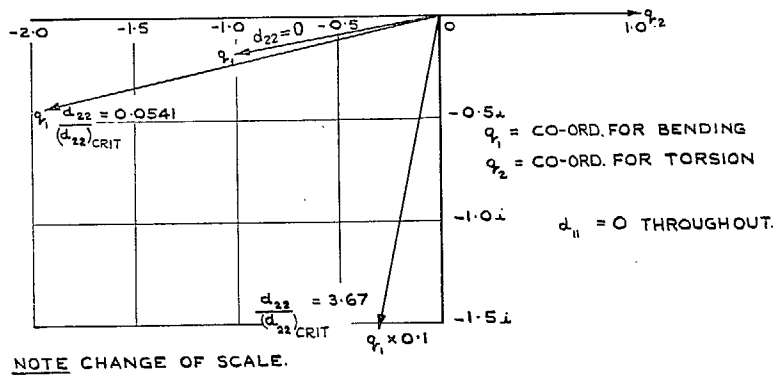


FIG. 10. Amplitude ratio ( $q_1/q_2$ ) for various values of structural damping (*Meteor* with tip mass).

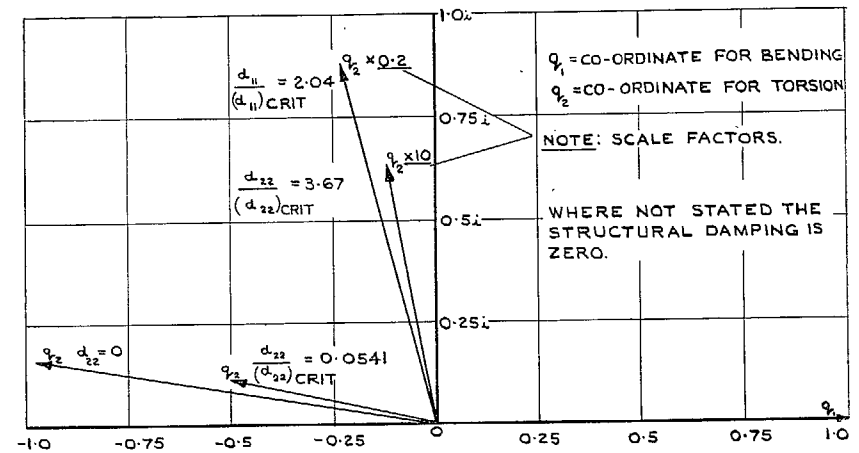


FIG. 11. Amplitude ratio ( $q_2/q_1$ ) for various values of structural damping (*Meteor* with tip mass).

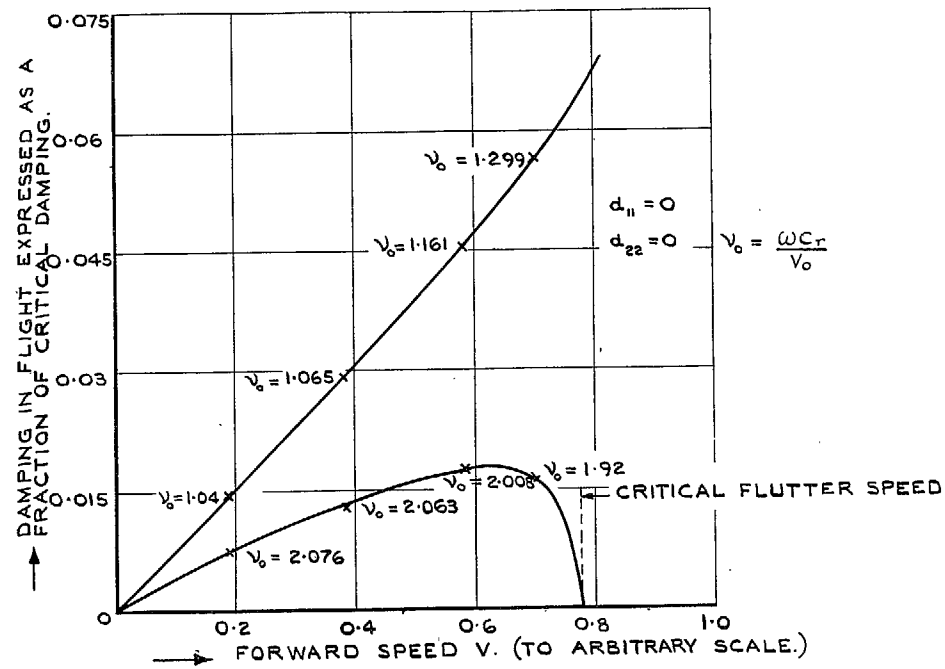


FIG. 12a. The variation of flight damping with speed for zero structural damping (*Meteor* with tip mass).

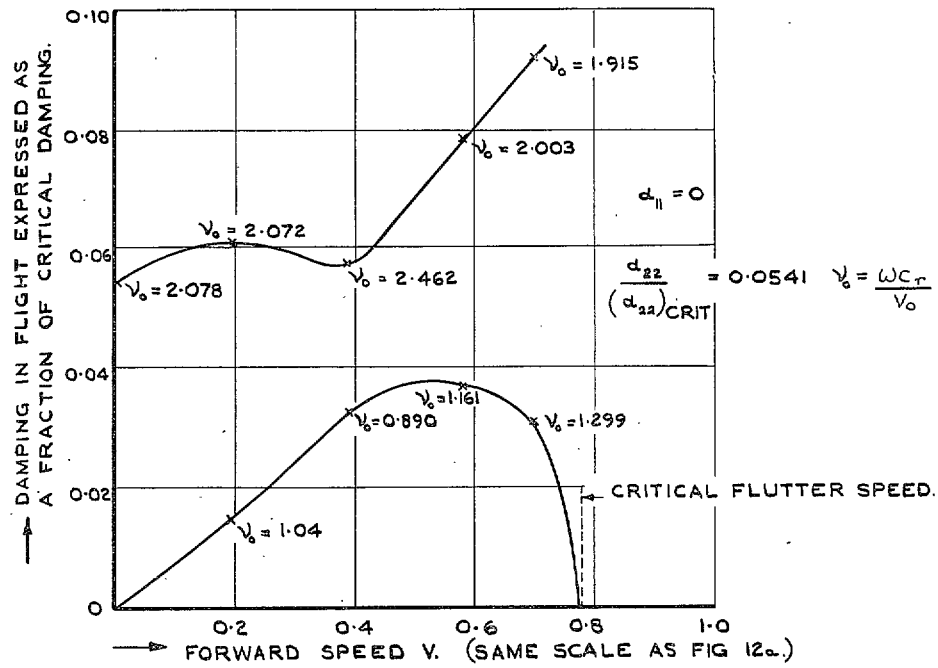


FIG. 12b. The variation of flight damping with speed for 5.4 per cent. critical structural damping (*Meteor* with tip mass).

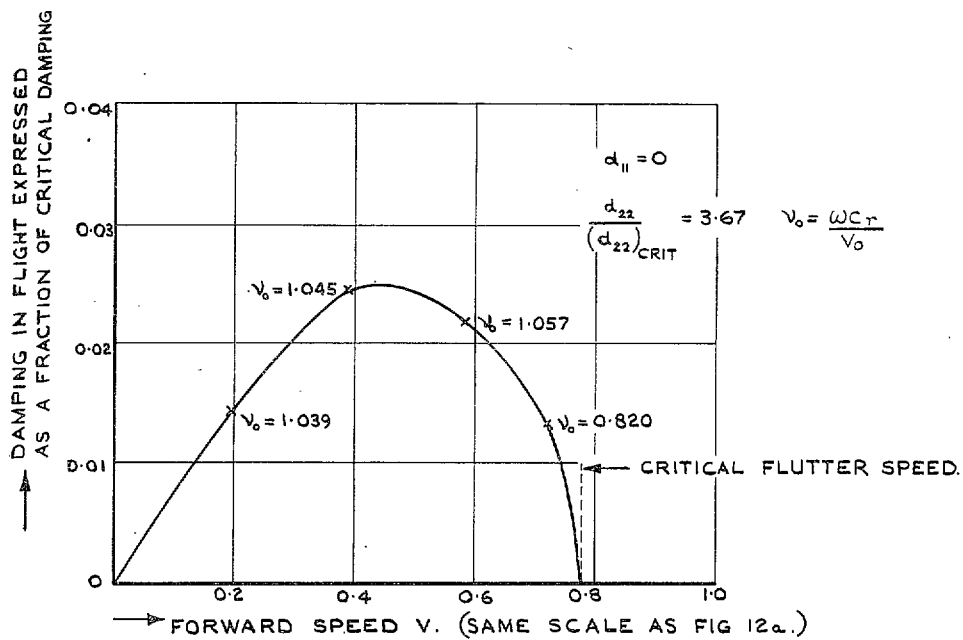


FIG. 12c. The variation of flight damping with speed, for 3.67 per cent critical structural damping (*Meteor* with tip mass).

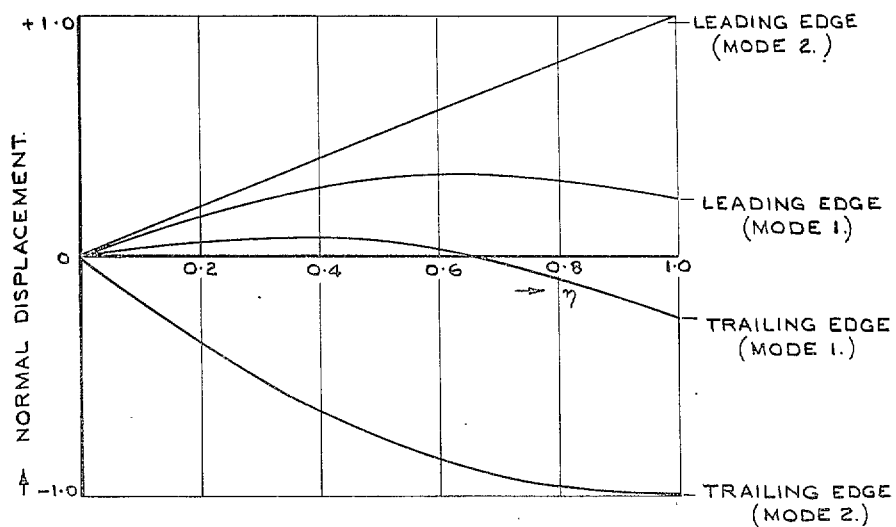


FIG. 13. Modes constructed to produce a fall in flutter speed when the structural damping was increased.

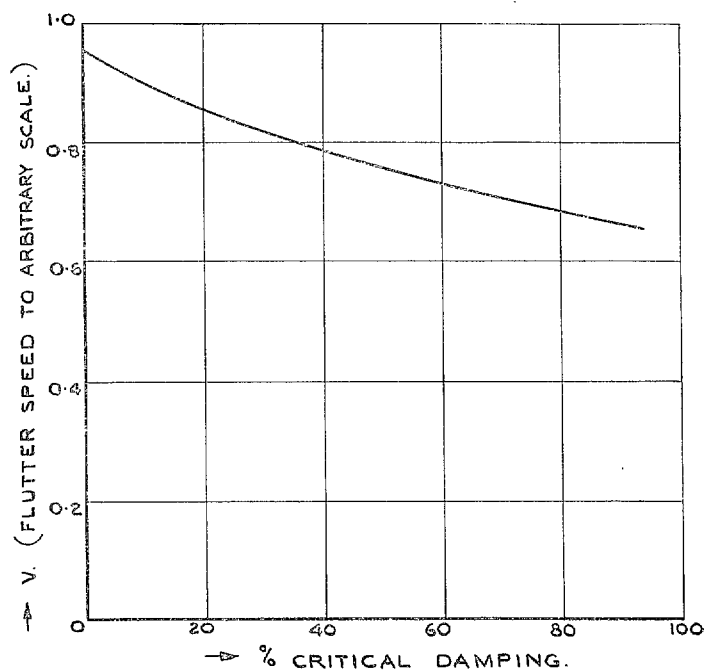


FIG. 14. Variation of flutter speed with torsional damping for a hypothetical wing having the modes of FIG. 13.

## Publications of the Aeronautical Research Council

### ANNUAL TECHNICAL REPORTS OF THE AERONAUTICAL RESEARCH COUNCIL (BOUND VOLUMES)

- 1939 Vol. I. Aerodynamics General, Performance, Airscrews, Engines. 50s. (52s.)  
Vol. II. Stability and Control, Flutter and Vibration, Instruments, Structures, Seaplanes, etc. 63s. (65s.)
- 1940 Aero and Hydrodynamics, Aerofoils, Airscrews, Engines, Flutter, Icing, Stability and Control, Structures, and a miscellaneous section. 50s. (52s.)
- 1941 Aero and Hydrodynamics, Aerofoils, Airscrews, Engines, Flutter, Stability and Control, Structures. 63s. (65s. 3d.)
- 1942 Vol. I. Aero and Hydrodynamics, Aerofoils, Airscrews, Engines. 75s. (77s. 3d.)  
Vol. II. Noise, Parachutes, Stability and Control, Structures, Vibration, Wind Tunnels. 47s. 6d. (49s. 3d.)
- 1943 Vol. I. Aerodynamics, Aerofoils, Airscrews. 80s. (82s.)  
Vol. II. Engines, Flutter, Materials, Parachutes, Performance, Stability and Control, Structures. 90s. (92s. 3d.)
- 1944 Vol. I. Aero and Hydrodynamics, Aerofoils, Aircraft, Airscrews, Controls. 84s. (86s. 6d.)  
Vol. II. Flutter and Vibration, Materials, Miscellaneous, Navigation, Parachutes, Performance, Plates and Panels, Stability, Structures, Test Equipment, Wind Tunnels. 84s. (86s. 6d.)
- 1945 Vol. I. Aero and Hydrodynamics, Aerofoils. 130s. (133s.)  
Vol. II. Aircraft, Airscrews, Controls. 130s. (133s.)  
Vol. III. Flutter and Vibration, Instruments, Miscellaneous, Parachutes, Plates and Panels, Propulsion. 130s. (132s. 9d.)  
Vol. IV. Stability, Structures, Wind Tunnels, Wind Tunnel Technique. 130s. (132s. 9d.)
- 1947 Vol. I. Aerodynamics, Aerofoils, Aircraft. 168s. (171s. 3d.)

### Annual Reports of the Aeronautical Research Council—

1939-48 3s. (3s. 5d.) 1949-54 5s. (5s. 5d.)

### Index to all Reports and Memoranda published in the Annual Technical Reports, and separately—

April, 1950 - - - - R. & M. 2600 6s. (6s. 2d.)

### Published Reports and Memoranda of the Aeronautical Research Council—

Between Nos. 2351-2449	R. & M. No. 2450 2s. (2s. 2d.)
Between Nos. 2451-2549	R. & M. No. 2550 2s. 6d. (2s. 8d.)
Between Nos. 2551-2649	R. & M. No. 2650 2s. 6d. (2s. 8d.)
Between Nos. 2651-2749	R. & M. No. 2750 2s. 6d. (2s. 8d.)
Between Nos. 2751-2849	R. & M. No. 2850 2s. 6d. (2s. 8d.)
Between Nos. 2851-2949	R. & M. No. 2950 3s. (3s. 2d.)

*Prices in brackets include postage*

### HER MAJESTY'S STATIONERY OFFICE

York House, Kingsway, London W.C.2; 423 Oxford Street, London W.1; 13a Castle Street, Edinburgh 2; 39 King Street, Manchester 2; 2 Edmund Street, Birmingham 3; 109 St. Mary Street, Cardiff; 50 Fairfax Street, Bristol 1; 80 Chichester Street, Belfast 1, or through any bookseller.